Research White Paper

WHP 161

July 2008

2-by-2 MIMO fixed reception channel model for dual-polar terrestrial transmission

P.N. Moss

BRITISH BROADCASTING CORPORATION

BBC Research White Paper WHP 161

2-by-2 MIMO fixed reception channel model for dual-polar terrestrial transmission

P.N. Moss

Abstract

In collaboration with Arqiva, NGW and OFCOM, BBC Research has recently set up an experimental 2-by-2 MIMO-DVB broadcast chain utilising a 2 x 250W ERP transmission from Guildford transmitting station, Surrey, UK. The transmitter is configurable into conventional DVB-T, dual-polar MIMO and co-polar MIMO modes. Survey work has been carried out using a vehicle equipped with a similarly configurable receiver, with the primary intention of comparing the coverage areas of the conventional and MIMO systems. A useful additional outcome of the campaign is the existence of logged impulse response data for the 2-by-2 MIMO channels allowing a provisional channel model to be proposed, albeit based on the limited data from a single transmitter. It is this latter task for the fixed-reception dual-polar case which forms the subject matter of this document.

Additional key words: none

White Papers are distributed freely on request.

Authorisation of the Head of Broadcast/FM Research is required for publication.

BBC Research White Paper WHP 161

2-by-2 MIMO fixed reception channel model for dual-polar terrestrial transmission

P.N. Moss

CONTENTS

This page is deliberately left blank

BBC Research White Paper WHP 161

2-by-2 MIMO fixed reception channel model for dual-polar terrestrial transmission

P.N. Moss

1 Introduction

In collaboration with Arqiva, NGW and OFCOM, BBC Research has recently set up an experimental 2-by-2 MIMO-DVB broadcast chain utilising a 2 x 250W ERP 730MHz transmission from Guildford transmitting station, Surrey, UK. The transmitter is configurable into conventional DVB-T, dual-polar MIMO and co-polar MIMO modes. Full technical details of a very similar (but lower power) system were published in a conference paper at IBC2006 [1], and more recently the work has been reported in a second IBC paper [9].

Survey work based on the Guildford transmitter has been carried out using a vehicle equipped with a configurable receiver, with the primary intention of comparing the coverage areas of the conventional and MIMO systems. An important additional outcome of the campaign is the existence of logged impulse response data for the 2-by-2 MIMO channels, allowing a provisional channel model to be proposed, albeit based on the limited data from a single transmitter. It is this latter task for the fixed-reception dual-polar case which forms the subject matter of this document.

The document is structured as follows. First, the general principles of channel modelling based on tapped delay lines are outlined. Next, existing models for DVB-T are very briefly described. Finally, the features of the measured MIMO channel are described and the corresponding 2-by-2 model developed.

2 Tapped delay line channel models

2.1 Structure

The basic structure of the model is shown in figure 1. The intention is to synthesise the target channel impulse response using an FIR structure with specified weights which may be fixed or allowed to vary in time if the channel Doppler behaviour is to be included.

Figure 1: Tapped Delay Line Model

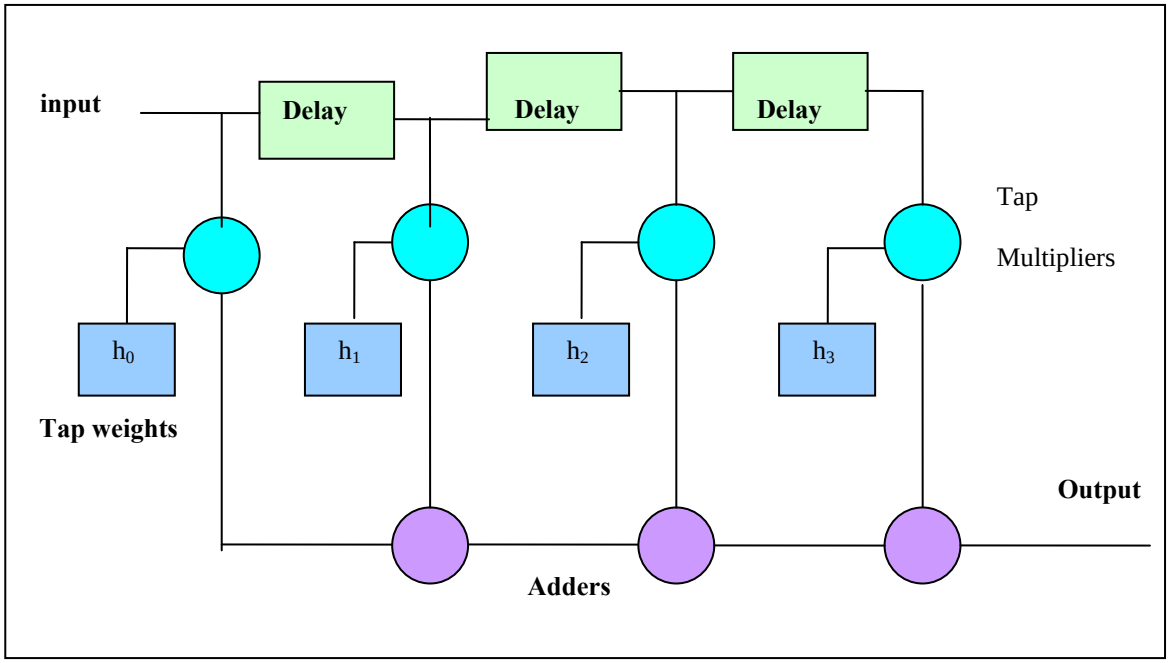

The impulse response generated by a structure with *N* taps at time *t* is given by

$$h(t,\tau) = \sum_{n=0}^{N-1} h_n(t)\delta(\tau - \tau_n) \quad \ldots\ldots(1)$$

$h_n(t)$ is the value of tap index *n* at time *t.* τ_n is the delay associated with that tap.

In addition, Gaussian noise is usually added at the output of the tapped delay line to represent the random noise present at the input of the receiver.

2.2 Tap spectra

If, as in equation (1), the taps in the model are time-varying then these will usually be stochastic in nature and characterised by a specified variance, PDF (probability density function) and PSD (power spectral density). Assuming a complex baseband form for the model, a popular choice for the distribution of the tap weights is complex Gaussian. It follows that the tap magnitude then has a Rayleigh distribution.

The PSD defines the 'Doppler spread' of the path and typically has either a 'Classical' , 'Gaussian' or 'Ricean' response shape. The 'Classical' PSD is given by

$$S(f) = \frac{A}{\sqrt{1-(f/f_d)^2}} \quad \ldots\ldots(2)$$

for

$$f \le f_d$$

f_d is a parameter controlling the maximum Doppler width. It is chosen to be proportional to an assumed vehicle speed. The 'Gaussian' PSD is of the form

$$G(A, f_1, f_2) = A\exp\left(\frac{-(f-f_1)^2}{2f_2^2}\right) \quad \ldots\ldots(3)$$

f_1 and f_2 are parameters controlling the width and offset of the distribution.

The width of the Doppler spectrum is usually very much less than the signal bandwidth. So at any given time, the tap weights can be considered fixed for the duration of the impulse response without introducing significant error.

The combination of Rayleigh PDF and specified PSD can be conveniently realised in simulation by feeding complex Gaussian noise into an appropriate filter.

The 'Ricean' PSD adds a pure-Doppler term to the path, e.g. in combination with a Classical spectrum it results in the following:

$$S_R(f) = \frac{A}{\sqrt{1-(f/f_d)^2}} + B\delta(f - \alpha f_d) \quad \ldots\ldots(4)$$

2.3 Tap correlation

The stochastic tap weights may be modelled as independent if the physical data suggests this. This assumption results in the simplest form of figure 1, with independent noise generators and spectral-shaping Doppler filters providing each time-varying tap weight. However, it may be necessary to introduce a degree of correlation between the taps, based on the observed correlation properties of the signal to be modelled. To achieve this, sufficient data must be processed to provide a good estimate of relevant statistical measures; in particular the covariance matrix of the vector formed from the values of the sampled impulse response. This matrix has a general term of the form

$$\mathbf{R_{nm}} = E\left\{h(\tau_n) \cdot h^*(\tau_m)\right\} \quad \ldots\ldots(5)$$

where $h(\tau_k)$ is the complex impulse response and (assuming ergodicity) the expectation can be evaluated over time at any given location.

If the tap vector has *N* elements, then it follows that **R** is a *N* x *N* Hermitian matrix.

Once **R** is known, it is necessary to arrange for the tapped delay-line model to exhibit an impulse response with the corresponding correlation properties. This is achieved by taking a vector of independent noise sources and applying a common Doppler filter to each element. The resulting noise vector is then pre-multiplied by a *transition matrix* (**V**) of appropriate properties. It can be shown that a suitable transition matrix is given by

$$\mathbf{V} = \mathbf{U}\mathbf{\Lambda}^{\frac{1}{2}} \quad \ldots\ldots(6)$$

where **U** is a unitary matrix made up of the eigenvectors of **R**, and **Λ** is a diagonal matrix made up of the eigenvalues of **R**. An alternative formulation is possible in terms of the Cholesky decomposition of **R**; it can be shown that the Hermitian transpose of the Cholesky decomposition is a suitable transition matrix.

2.4 Power delay profile and delay spread

The diagonal values of $\mathbf{R}_{nm}$ define the *power delay profile* (PDP) of the channel, according to the equation

$$P_i = \mathbf{R}_{ii} \quad \ldots\ldots(7)$$

For a particular impulse response made up of N discrete samples the delay spread is defined as the *standard deviation of (power-weighted) delay* in accordance with the following equation:

$$SD_j = \sqrt{\frac{\sum_i P_i \cdot \tau_i^2}{\sum_i P_i} - \left(\frac{\sum_i P_i \cdot \tau_i}{\sum_i P_i}\right)^2} \quad \ldots\ldots(8)$$

3 Existing channel models for DVB-T and DVB-H

3.1 Overview

Various models of the single-in, single out (SISO) channel exist which could be considered as a basis for a MIMO channel model. These are outlined below.

3.2 Gaussian

The Gaussian channel simply adds Gaussian noise to the attenuated transmitted signal, without frequency selectivity. It is hence a 'one-tap' model characterised simply by a signal-to-noise ratio. It represents only certain idealised propagation conditions but is useful for receiver testing.

3.3 COST207

The COST207 programme was funded by the European Commission in the 1980s and studied channel models in the UHF bands primarily for mobile cellular applications. Multi-tap models were proposed for rural and urban environments and two examples are shown below.

3.3.1 Typical Rural (RA)

Table 1: Six-tap Rural Model

Tap	Delay(μs)	Relative power (dB)	Doppler spectrum
1	0	0	Ricean[1]
2	0.1	-4	Classical
3	0.2	-8	Classical
4	0.3	-12	Classical
5	0.4	-16	Classical
6	0.5	-20	Classical

3.3.2 Typical Urban (TU)

Table 2 :Six-tap Urban Model

Tap	Delay(μs)	Relative power (dB)	Doppler spectrum
1	0.0	-3	Classical
2	0.2	0	Classical
3	0.5	-2	Gaus1[2]
4	1.6	-6	Gaus1
5	2.3	-8	Gaus2[3]
6	5.0	-10	Gaus2

3.4 ETSI EN300 744 DVB-T

Annex B of ETSI document EN300 744 [5] defines models for fixed and portable reception. The difference between them is that the model for fixed reception includes a line-of-sight (LOS) term in addition to the twenty delayed taps shown here. The LOS term for fixed reception has a total power 10dB greater than that of all the other taps (i.e. Ricean K =10). No time variation of the taps is included, so there is no associated Doppler profile.

Table 3: ETSI 20-tap Model

Tap	Delay(μs)	magnitude	Phase(rad)
1	0.073883	0.225894	2.128544
2	0.143556	0.15034	3.952093
3	0.153832	0.051534	1.093586
4	0.194207	0.149723	3.462951
5	0.203952	0.170996	1.099463
6	0.429948	0.295723	5.928383
7	0.51865	0.407163	5.86447
8	0.602895	0.258782	3.758058
9	0.640512	0.221155	3.33429
10	0.848831	0.262909	0.628578
11	0.92445	0.24014	3.664773
12	1.003019	0.057662	4.855121
13	1.016585	0.061831	5.430202
14	1.368671	0.25973	0.393889
15	1.38132	0.116587	2.833799
16	1.93557	0.400967	0.154459
17	2.751772	0.303585	2.215894
18	3.228872	0.350825	3.053023
19	3.324866	0.185074	5.775198
20	5.422091	0.176809	3.419109

[1] Ricean has $A=0.41/2\pi f_d$ $B=0.91$

[2] Gaus1 has two Gaussian components: first is $A=1;f_1=-0.8f_d;f_2=0.05f_d$ second is $A=0.1;f_1=+0.4f_d;f_2=0.1f_d$

[3] Gaus2 has two Gaussian components: first is $A=1;f_1=+0.7f_d;f_2=0.1f_d$ second is $A=0.0316;f_1=-0.4f_d;f_2=0.15f_d$

3.5 Wing-TV DVB-H

The Wing-TV project introduced new models for portable reception of DVB-H, prompted by the need for improved accuracy over COST207 models. Two main variants were devised, for portable indoor and portable outdoor reception. The following tables were derived from [3].

3.5.1 Portable indoor

Table 4: Portable Indoor Model

Tap	Delay(μs)	Power(dB)	Doppler Spectrum	fd(Hz)
1	0.0	0.0	G(0.1,0,0.08fd)+δ(f-0.5fd)	1.69 (=3km/h 666MHz)
2	0.1	-6.4	G(1,0,0.08fd)	1.69
3	0.2	-10.4	G(1,0,0.08fd)	1.69
4	0.4	-13.0	G(1,0,0.08fd)	1.69
5	0.6	-13.3	G(1,0,0.08fd)	1.69
6	0.8	-13.7	G(1,0,0.08fd)	1.69
7	1.0	-16.2	G(1,0,0.08fd)	1.69
8	1.6	-15.2	G(1,0,0.08fd)	1.69
9	8.1	-14.9	G(1,0,0.08fd)	1.69
10	8.8	-16.2	G(1,0,0.08fd)	1.69
11	9.0	-11.1	G(1,0,0.08fd)	1.69
12	9.2	-11.2	G(1,0,0.08fd)	1.69

3.5.2 Portable outdoor

Table 5: Portable Outdoor model

Tap	Delay(μs)	Power(dB)	Doppler Spectrum	Fd(Hz)
1	0.0	0.0	G(0.1,0,0.08fd)+δ(f-0.5fd)	1.69 (=3km/h 666MHz)
2	0.2	-1.5	G(1,0,0.08fd)	1.69
3	0.6	-3.8	G(1,0,0.08fd)	1.69
4	1.0	-7.3	G(1,0,0.08fd)	1.69
5	1.4	-9.8	G(1,0,0.08fd)	1.69
6	1.8	-13.3	G(1,0,0.08fd)	1.69
7	2.3	-15.9	G(1,0,0.08fd)	1.69
8	3.4	-20.6	G(1,0,0.08fd)	1.69
9	4.5	-19.0	G(1,0,0.08fd)	1.69
10	5.0	-17.7	G(1,0,0.08fd)	1.69
11	5.3	-18.9	G(1,0,0.08fd)	1.69
12	5.7	-19.3	G(1,0,0.08fd)	1.69

4 The measurement campaign

4.1 Overview

The measurement campaign was centred on an experimental 2 x 250W ERP transmission from Guildford transmitter site, with antennas at 45m AGL (dual-polarised) and 32m (horizontal). In the dual-polarised MIMO mode, only the 45m antennas were used. For co-polar measurements, the horizontal antenna at 45m was to be excited together with the horizontal antenna at 32m. The site landlord was National Grid Wireless (NGW) who provided accommodation for the transmitter equipment bay and antenna rigging effort. The equipment bay itself was initially commissioned at Emley Moor (Arqiva) using a BBC Research experimental exciter and proprietary power amplifiers and channel filters. Compliance with the non-critical DVB-T spectral mask was observed.

The receiving antennas for 10m were van-mounted on a pump-up mast and comprised a pair of Yagi antennas with about 11.5dBi gain.

All parties mentioned, along with OFCOM, were working as part of the Advanced Terrestrial Transmission Study Group (ATTSG) chaired by the BBC.

The campaign lasted about 12 months, intermittently, and surveyed around 50 sites at 10m, with additional data gathered at 1.5m (portable

5 Proposed model for fixed 10m reception of 2-by-2 MIMO

5.1 General approach

The aim is to provide a model of paths shown as $h_{11}, h_{12}, h_{21}, h_{22}$ in figure 2 below, where Tx1 and Tx2 represent twin antennas at a terrestrial transmitter site and Rx1 and Rx2 the two elements of a MIMO receive antenna whether fixed or mobile.

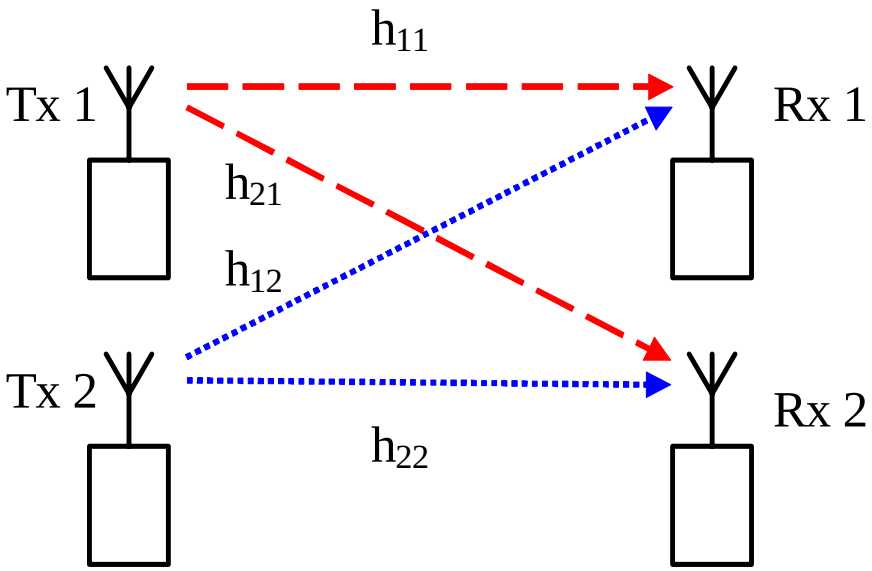

Figure 2 - 2-by-2 MIMO system

The simplest approach to the MIMO case is to start with one of the existing DVB-T models described earlier and assume it can be used to model each of the four transmission paths $h_{11}, h_{12}, h_{21}, h_{22}$. The task of the MIMO modelling exercise is then to quantify the statistical relationship between these four terms. However it was decided to first produce an independent model of the channel behaviour observed during the measurement campaign, without excluding the possibility of simply augmenting existing models from the present MIMO propagation data if desired.

An 18-tap model of the propagation paths was chosen, with the first four taps spaced at one-quarter of the interval of the next 14. This was to capture more detail in the low excess delay region whilst keeping the total number of taps required to encompass the observed delay spread reasonably low. The tap spacings are 263ns and 1.053μs respectively for the two regions, numbers that result from the existence of 142 DVB-T pilots in a 7.6MHz interval (See appendix 1 for details of the pilot processing and tap temporal positions). In the proposed model, the first 'fine' tap is the sum of a line-of-sight term and a Rayleigh distributed term. It hence has a Ricean distribution. The remaining 17 taps are drawn from a Rayleigh distribution. The overall power delay profile (PDP) is scaled so that the total impulse response power is unity[4,5] Now each path in of the model $h_{11}, h_{12}, h_{21}, h_{22}$ is of this multi-tap structure and is characterised by a Ricean K-factor value and a PDP These quantities must be determined from the data. A Ricean distribution describes stochastic data which is the sum of constant term and a Rayleigh distributed term. The power ratio of the two is known as the Ricean K-factor.

[4] For the terms h_{11}, h_{22}. For terms h_{12}, h_{21}, the procedure is initially followed then finally re-scaled in accordance with the measured ratio of co-polar to cross-polar power.
[5] The term 'total impulse response power' means the sum of the powers of the PDP elements.

Generalising to the MIMO case replaces each tap with a set of four taps, representing the matrix elements at 18 distinct time points. For each of the purely Rayleigh-fading taps (i.e. indices 2-18), and the Rayleigh component of the first tap, a 4-by-4 matrix **R** can be deduced to describe the cross-correlation of the stochastic tap weights. The diagonal entries of the *k*th tap are proportional to the 4-term PDP of that tap, i.e. at the *k*th time point. The off-diagonal entries are proportional to the correlation between matrix elements, again at the *k*th time point. It is assumed that the Rayleigh component of the first tap (index 1) is described by a similar cross-correlation matrix.

Mathematically we can express the proposed channel model as

$$\mathbf{vec}(\mathbf{H}^T(t)) = \mathbf{L}\delta(t) + \sum_{j=1}^{18} \mathbf{R}_j^{1/2}\mathbf{x}_j\delta(t-\tau_j) \quad \ldots\ldots\ldots\ldots\ldots\ldots\ldots\ldots (9)$$

$$\text{where } \mathbf{vec}(\mathbf{H}^T) = \begin{pmatrix} h_{11} \\ h_{12} \\ h_{21} \\ h_{22} \end{pmatrix}, \ \mathbf{L} = \begin{pmatrix} \sqrt{\frac{K_{11}}{1+K_{11}}} \exp j\theta_{11} \\ \sqrt{\frac{K_{12}}{1+K_{12}}} w_{12} \exp j\theta_{12} \\ \sqrt{\frac{K_{21}}{1+K_{21}}} w_{21} \exp j\theta_{21} \\ \sqrt{\frac{K_{22}}{1+K_{22}}} \exp j\theta_{11} \end{pmatrix} \quad \ldots\ldots (10)$$

where *t* is the time index and τ_j the time position of the *j*th tap (zero for *j*=1). K_{ij} are the Ricean K-factors for each term and θ_{ij} are uniformly distributed random phases. This form of **L** ensures the total impulse response power in h_{11}, h_{22} is unity and the w_{12}, w_{21} terms[6] adjust the LOS level appropriately for h_{12}, h_{22}. $\mathbf{R}_j$ is the 4-by-4 covariance matrix of the vectorised elements of the channel matrix at the j^{th} tap[7]. $\mathbf{x_j}$ is a (distinct) random vector for each *j* with i.i.d. complex Gaussian components of unit variance. The required square root of $\mathbf{R}_j$ satisfies $\mathbf{R} = \mathbf{R}^{1/2}\mathbf{R}^{*/2}$ is extracted using equation (6), where it is equal to **V**, or by taking the Cholesky decomposition of $\mathbf{R}_j$ and then taking the Hermitian transpose.

The description of the model so far is for a 'one-off' channel realisation; we obtain a set of tap values from the stated probability distributions. For fixed reception, the intention is to model the system with many such 'fixed' channel responses in order to evaluate the performance.

Having decided on the general form of the model, the next task was to obtain the parameters of the model pertinent to each transmit/receive scenario from the measured data. The results of this procedure are discussed below.

5.2 Data analysis

The data was gathered using continuous pilot captures of 160-640[8] down-sampled symbol-quads taking groups of four contiguous pilot phases (p1 p2 p3 p4) at regular intervals[9] whilst the 10m mast was slowly shunted at around 0.5m/s.

---

[6] $w_{12} = w_{21}$ in this model

[7] Excluding line-of-sight terms; i.e. the Rayleigh fading part of tap one and the whole of all other taps

[8] Typically 1-4 'shunts' of 160 captures

[9] Taking symbols 1,2,3,4,541,542,543,544 etc

5.2.1 Averaged Power Delay Profiles (PDP)

Averaging over a total of 35 shunts at 16 locations produced the following plots showing the 18-tap profiles of the principal components (h_{11}, h_{22}) and the cross terms (h_{12}, h_{21}). The average PDP[10] obtained at each location was normalised such that the taps summed to unity and an overall average PDP then calculated.

Figure 3: Averaged power delay profiles (Fixed)

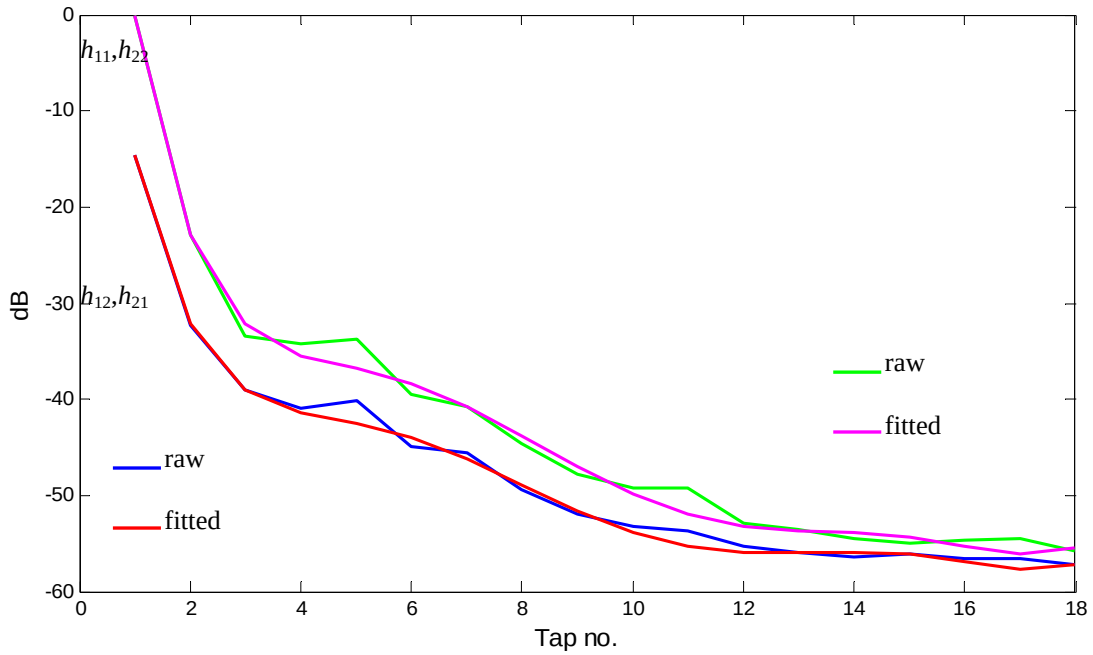

For both pairs of terms, the raw data is plotted together with a least-squares sixth-order function fit calculated in MATLAB. The final values of the modelling procedure are obtained by taking the function fit as a starting point but restoring the pre-fitted values to the tap 1 terms and to the *sum* of terms 2-18. From the plot, and the original high-resolution source data, it can be seen that the cross-polar coupling associated with the LOS-containing component (tap 1) is about 15dB whereas it is approximately 8-10dB for the earliest delayed taps.

5.2.2 Averaged covariance matrix Rav

Analysing over the same sets of location data produced the following correlation matrix $\mathbf{R}_{av}$. It was found by taking an overall mean of the individual correlation matrices $\mathbf{R}_j$ of taps 2-18 at each location, then normalising the largest term to unity. After that, the mean of all the normalised location matrices was taken.

$$\mathbf{R}_{av}=\begin{pmatrix} 0.70543 & 0.05105 & 0.01769 & 0.1382 \\ 0.05105 & 0.08276 & 0.004946 & 0.02641 \\ 0.01769 & 0.004946 & 0.11418 & 0.03480 \\ 0.13821 & 0.02641 & 0.03480 & 0.9578 \end{pmatrix} \quad \ldots\ldots\ldots\ldots\ldots\ldots\ldots\ldots\ldots\ldots (11)$$

The leading diagonal of this matrix has terms proportional to the average power[11] of each channel coefficient h_{11}, h_{12}, h_{21} and h_{22} respectively. The other two corner terms, which are relatively high, show a correlation between h_{11} and h_{22} which is presumably due commonalities in their scattering environment. Other terms are, however, quite small.

For the purposes of the model, the following simplified matrix is proposed for the j^{th} tap:

[10] Within a location, the shunts were concatenated without any normalisation in deriving the PDP.
[11] of the Rayleigh terms, not the LOS terms

$$\mathbf{R}_j(1,1)\begin{pmatrix} 1 & 0.125\sqrt{X_j} & 0 & 0.15 \\ 0.125\sqrt{X_j} & X_j & 0 & 0 \\ 0 & 0 & X_j & 0.125\sqrt{X_j} \\ 0.15 & 0 & 0.125\sqrt{X_j} & 1 \end{pmatrix} \quad \text{(12)}$$

Small terms (cutoff 0.03) have now been zeroed. The value of X_j is set at each tap position equal to the average[12] ratio of cross-term (h_{12}, h_{21}) to principal term (h_{11}, h_{22}) power[13]. The multiplier $\mathbf{R}_j(1,1) = \mathbf{R}_j(4,4)$ is the principal term power level at the j^{th} tap.

5.2.3 Doppler spectrum

The model for fixed reception provides fixed taps drawn from underlying stochastic processes each time it is instantiated. So there is no Doppler variation within a simulation (although there may be many sub-simulations each with distinct taps if desired).

5.2.4 K-factor

The K-factor was estimated using the method of moments [7], which first evaluates the second and fourth moments of the frequency response data along the t-axis[14]. From this, the K-factor of an assumed underlying Ricean distribution may be deduced. The distribution function was not independently confirmed as Ricean, but future work could perhaps address this when time permits by employing the Kolmogorov-Smirnov significance test [8]. However, even in the absence of such verification, or in the consequent knowledge that the spatial distribution is not Ricean, the K-factor remains a useful comparative measure.

The measurements showed that in many cases the spatial variation along a shunt was indicative of a strong line-of-sight (LOS) component on the principal matrix terms (h_{11}, h_{22}) and hence a high Ricean K-factor. However, there were also many shunts where this was not the case due to scattering and partial path blocking. Our final model for 10m reception must reflect these observations and allow for a range of spatial K-factors.

For illustration, the plots below show typical shunt power variation for high, medium and low-K scenarios. The actual K-values for h_{11}, h_{22} are approximately 20, 4.3 and 1.1 respectively.

The x-axis label refers to downsampled symbol-quad number, as described above in para 5.2. One in 135 such quads is outputted from the downsampling process.

[12] At the particular tap i.e. $(|h11|^2+|h22|^2)/(|h12|^2+|h21|^2)$
[13] For the first tap, the appropriate ratio is the Rayleigh component of the principal terms to that of the cross-terms.
[14] i.e. we examine the evolution in time of each frequency bin and assign a K to each, from which an overall K is deduced. The frequency domain allows a better estimate of K since it is nominally flat; the ‘impulsive’ nature of the impulse response makes K-estimation in this domain highly prone to errors from FFT window ‘judder’ compromising accuracy.

Figure 4A: Typical variation of |H|2 at high-K location: Riverside

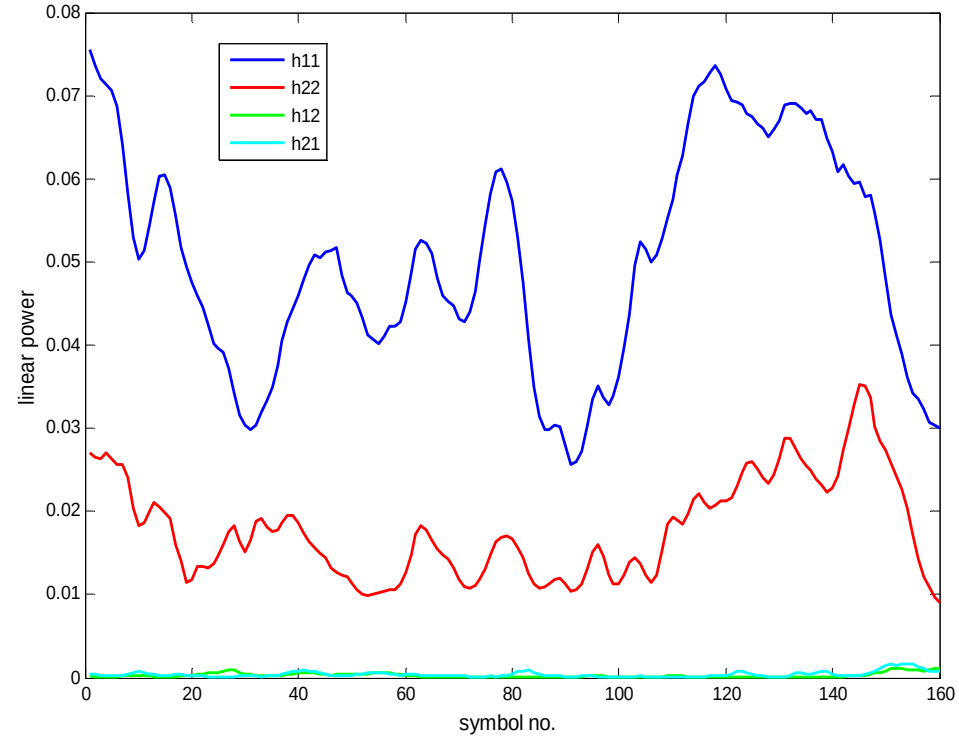

Figure 4B: Typical variation of |H|2 at medium-K location: Burpham

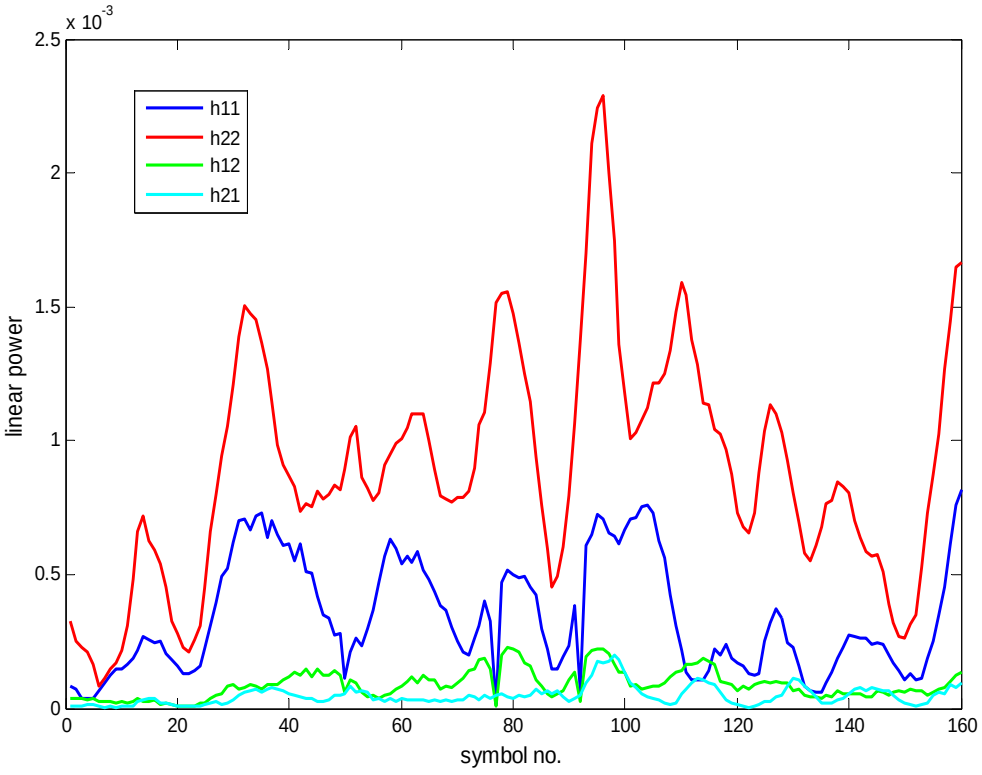

Figure 4C: Typical Low-K location: Whitemore Road

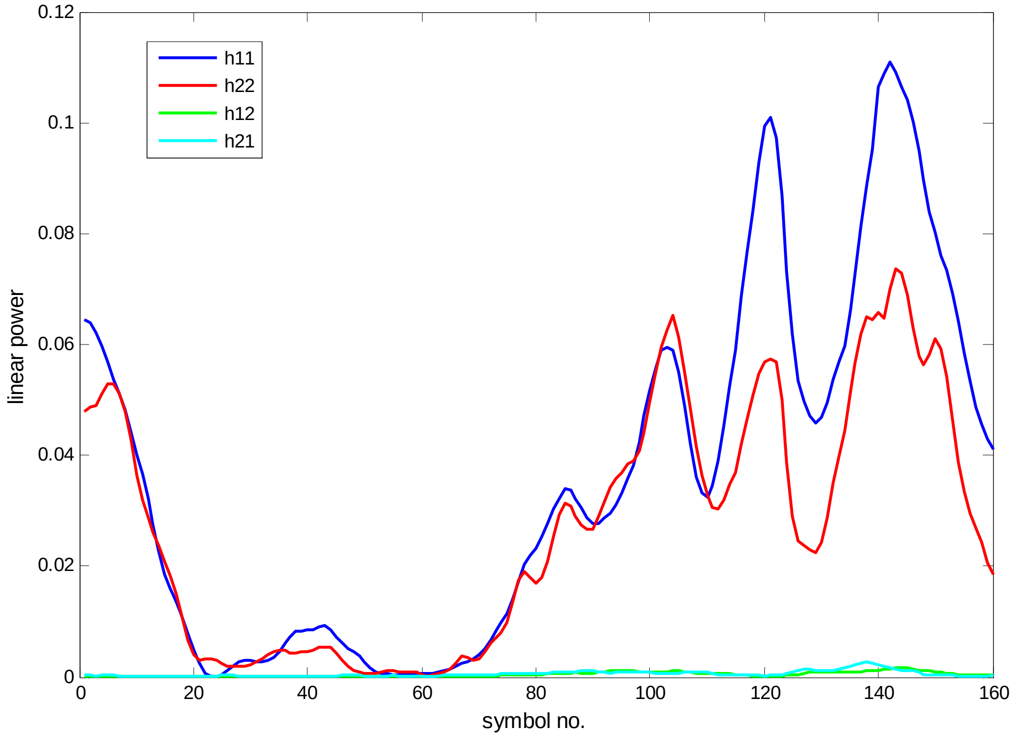

In almost all cases the cross terms (h_{12}, h_{21}) were characterised by a lower K-factor than that of the principal terms. This is not surprising and the cross-polar discrimination will tend the reject the LOS path and thereby give a relative boost to skew-polarised Rayleigh-distributed reflections.
Given the observed wide variation of K, it is recommended that for system simulations the tap values to be defined below are used in conjunction with K factors of 20, 5 and 1 for the principal terms and 3, 1 and 0 for the cross terms. The K factor is adjusted without varying the PDP by choosing the relative powers of the LOS and Rayleigh components of the first tap appropriately.

5.2.5 Partitioning the tap 1 power

For a chosen simulation K-factor it is necessary to partition the tap 1 power appropriately into a fixed LOS component and a Rayleigh distributed component. Because we have normalised the total energy in the principal terms to unity, their LOS component is given by:

$$L_1^2 = L_4^2 = \frac{K}{K+1} \dots\dots\dots (13)$$

The Rayleigh component of the first tap $\mathbf{R}_1(1,1)$ is hence

$$\mathbf{R}_1(1,1) = \frac{1}{K+1} - \sum_{j=2}^{18} \mathbf{R}_j(1,1) \dots\dots\dots (14)$$

Equations (13) and (14) provide $L_1 = L_4$, $\mathbf{R}_1(1,1)$ and $\mathbf{R}_1(4,4)$ since $\mathbf{R}_1(4,4) = \mathbf{R}_1(1,1)$.

For the cross terms $\mathbf{R}_1(2,2)$ and $\mathbf{R}_1(3,3)$,an analogous procedure to the above is followed to partition the tap 1 power, remembering that the RHS of (13) and the first term of the RHS of (13) must be scaled down by the overall cross power ratio XP:

$$L_2^2 = L_3^2 = \frac{K}{(K+1)XP} \quad \text{.....(15)}$$

The Rayleigh component of the first tap $\mathbf{R}_1(2,2)$ is hence

$$\mathbf{R}_1(2,2) = \frac{1}{(K+1)XP} - \sum_{j=2}^{18} \mathbf{R}_j(2,2) \quad \text{.....(16)}$$

Equations (15) and (16) provide L_2=L_3, $\mathbf{R}_1(2,2)$ and $\mathbf{R}_1(3,3)$ since $\mathbf{R}_1(3,3) = \mathbf{R}_1(2,2)$.

Once these four diagonals are known, the overall matrix (12) can be constructed for the Rayleigh part of the first tap.

5.2.6 Proposed tap values of the model

The entries below in table 6 have been deduced by employing the sixth-order fitting function followed by restoration of the pre-fitted values to the tap 1 terms and to the *sum* of terms 2-18. The term 1 power must split into LOS and Rayleigh as detailed above in para. 5.2.5 once the particular K-value for a simulation has been chosen. The tabulated data, taken together with equation (9) and covariance matrix (12), is the complete description of the model.

Table 6: Model for fixed (10m) reception

Tap number	$\lvert h_{11}\rvert^2, \lvert h_{22}\rvert^2$	$\lvert h_{12}\rvert^2, \lvert h_{21}\rvert^2$	**Notes**
			All terms dB
1	-0.029042 dB	-14.638 dB	
2	-22.82	-32.092	
3	-32.119	-38.937	
4	-35.436	-41.331	
5	-36.833	-42.482	
6	-38.366	-43.937	
7	-40.728	-46.129	
8	-43.791	-48.842	
9	-47.041	-51.579	
10	-49.904	-53.839	
11	-51.979	-55.308	
12	-53.16	-55.946	
13	-53.652	-55.999	
14	-53.888	-55.908	
15	-54.341	-56.129	
16	-55.231	-56.865	
17	-56.124	-57.705	
18	-55.439	-57.167	
rms delay spread	160ns	600ns	

It is apparent from the results that for most purposes a shortened 8-tap version of the model may be used since all principal terms beyond this are more than 45dB down. Indeed, measurement system noise probably accounts for part of the remaining terms.

The concentration of the impulse response energy into short times is believed to be due to the high-gain directional antennas used; long delay off-axis reflections are effectively suppressed. Hence the observed short delay spread values.

6 Conclusions and recommendations for further work

A provisional 2-by-2 MIMO model for the dual-polarised UHF broadcast channel has been presented for fixed 10m reception. The model has been based on a limited set of measurements taken from an experimental broadcast MIMO transmitter. The proposed power delay profile, correlation matrix and K-factors for simulation have been discussed.

The MIMO model presented may also find application in SISO, SIMO and MISO (e.g. Alamouti) simulations. To further support the latter, a short campaign of co-polar measurements is also recommended.

It is recommended that similar models are developed for portable and mobile reception, the latter including the time-varying behaviour.

7 References

[1] International Broadcasting Convention IBC2006 conference paper “A dual polarisation MIMO broadcast TV system” J.D. Mitchell, P.N.Moss and M.J.Thorp.

[3] Pekka Talmola, Erik Stare ‘DVB-T2 channel models’ DVB-T2 Draft document 2006-10-13

[4] European Commision, 1989, EUR12160 COST 207 “Digital Land Mobile Communications” 385 pages

[5] ETSI EN300 744 “Digital Video Broadcasting (DVB); Framing structure, channel coding and modulation for digital terrestrial television”.

[7] "On the estimation of the K parameter for the Rice fading distribution "Ali Abdi, Student Member, IEEE, Cihan Tepedelenlioglu, Student Member, IEEE, Mostafa Kaveh, Fellow, IEEE, and Georgios Giannakis, Fellow, IEEE Dept. of Elec. and Comp. Eng., University of Minnesota

[8] http://en.wikipedia.org/wiki/Kolmogorov-Smirnov_test

[9] International Broadcasting Convention IBC2007 conference paper “MIMO for broadcast – results from a high-power UK trial” J. Boyer, P.G Brown, K. Hayler, M. Lopez Garcia, J.D. Mitchell, P.N.Moss and M.J.Thorp.

Appendix 1: Pilot interpolation, post-processing and tap spacing details

Quasi-static channels:

Channel sounding of the 2-by-2 MIMO system is performed in conjunction with the actual MIMO/DVB-T signal by capturing the pilots from the two receiver halves and carrying out off-line MATLAB processing. To facilitate this, the experimental receiver writes the values of the scattered pilots on each of its two inputs to disc. In DVB-T 2k mode, there are four phases of pilots, as shown below, with 142 pilots in each (except the first phase which has 143; the last one is discarded.)

Figure A1-1: position of DVB-T scattered pilots

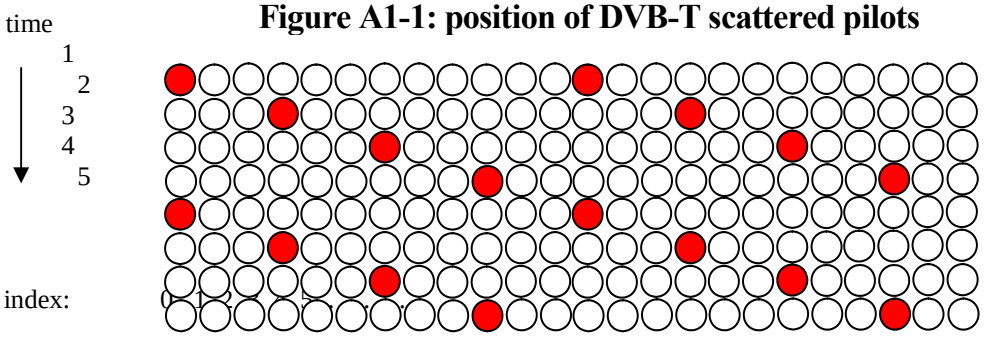

Only one in three carriers is ever a pilot, i.e. 568 in total (ignoring the highest-indexed carrier). At each measurement point either 4 or 64 symbols are captured[15], the former representing one on each pilot phase, the latter 16 on each phase. Except for calibration, measurements are not made on successive groups of four symbols since during a slow shunt the data would be strongly correlated.[16] Instead, the captures are on symbols 1,2,3,4,541,542,543,544,1081,1082,1083,1084…. etc[17]. The measurement points are grouped as 80,160,240 or 320 such 'quads' per shunt, and typically 1-4 shunts per location. In the post-processing MATLAB file the pilot data from each measurement point is placed initially in (e.g.) a 142 x 160 x 3 x no._locations x 4, the last dimension representing the four phases at that measurement point. Next they are upsampled along the first dimension, from 142 to 568 and placed appropriately for their phase as shown in figure A1-2. Such an array is written for both the A and B MIMO receiver halves (these are horizontal and vertical channels for a dual-polarisation system).

Figure A1-2: pilot organisation for post-processing

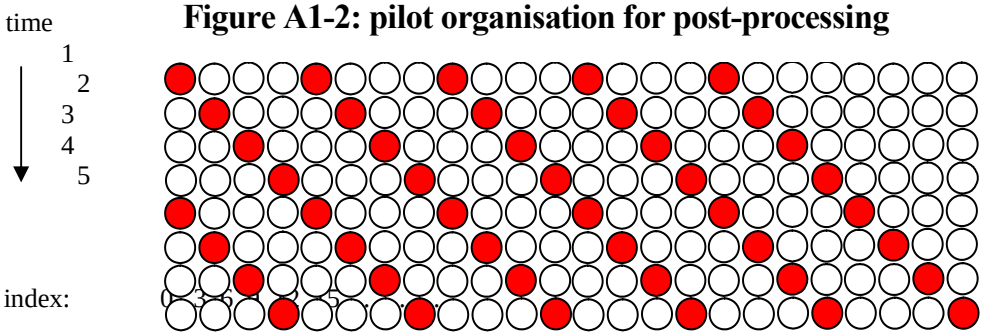

Of course, the pilots also differ from a strictly DVB-T pattern in that the transmitted pilots from one of the antennas are inverted on every other symbol. This means that, in the above diagram, phases 1 and 3 correspond to the channel sum and phases 2 and 4 to the channel difference. First we add these phase pairs together (1 addition for sum, 1 for difference for data and 16 additions for sum, 16 for difference for calibration to benefit from averaging). This procedure

[15] For data, one set of 4 for each measurement on each of A_chan and B_chan, the two antenna inputs to the receiver. For calibration data, one set of 64 for each of A_chan and B_chan.
[16] And hence a huge amount of data would be needed to have statistical significance.
[17] The channel is regarded as stationary over each 'quad' at shunt speed of 0.5m/s.

results in the structure of figure A1-3. But before we can add and subtract these quantities to obtain all the channel matrix components we must interpolate both sets of data (sum, difference) to obtain the full 568 values of each, as figure A1-4. We will still have only half that number of independent data points, of course, since interpolation adds no new information. This has consequences in our interpretation of the valid timespan of our impulse response output, as we shall see.

Figure A1-3: position of sum & difference pilots pre-interpolation

Sum

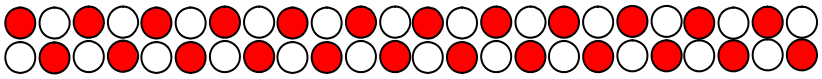

Difference

Figure A1-4: position of sum & difference pilots post-interpolation

Sum

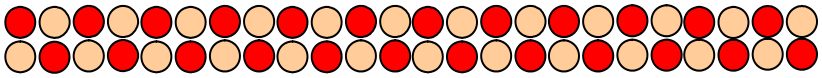

Difference

In A1-4 the lighter (tan) coloured positions represent interpolated data.

Next the required sum and difference operations are carried out to obtain the channel matrix entries $h_{11}, h_{12}, h_{21}, h_{22}$. At this point each term is represented by 568 points across the 7.6MHz interval. A 568-point DFT in now applied to generate an equivalent impulse response vector for each term $t_{11}, t_{12}, t_{21}, t_{22}$. A Hann window was chosen to give a reasonable compromise between main lobe width, substantially containing a LOS term in just two bins, and sideband level, which needed to allow for a 30-40dB dynamic range.

The sampling interval is 1/7.6MHz = 131.58ns and the time duration 74.74μs. Note, however, that the previously discussed interpolation means the potentially unambiguous length of the recovered impulse response (284 samples) corresponds to half that, i.e. 37.4μs (+/-18.7μs). In the code 160 samples (+21.1μs/-0μs) are initially retained, with the strongest overall term placed on the extreme left of this vector (index 1).

Next the 160 samples forming the shortened time vectors $st_{11}, st_{12}, st_{21}, st_{22}$ are mapped to the final 18-tap model as follows. The first eight components are paired and summed to form the first four 'finely spaced' terms of the 18-tap model with 263.2ns spacing. The next 112 components are grouped into blocks of eight and summed, giving 14 more 'coarsely spaced' taps with an interval of 1.053μs. The intermediate spacing between the last of the fine taps and the first of the coarse is 1053-1.5(263.2) = 658.2ns. The remaining 40 taps of the 160 are discarded as they are near the extreme of the useful impulse response as discussed above.

The MATLAB code outputs vectors (*model_1122* and *model_1221*) which are scaled to sum to unit power[18]. *Model_1122* describes the PDP of the principal terms h_{11}, h_{22} and *model_1221* describes the cross terms h_{12}, h_{21}. It was clear from the 'method of moments' K-factor analysis that the first tap could not realistically be described as completely line-of-sight, which would have been a useful simplification, but must have a Rayleigh component of its own. It follows that we must choose the true LOS and Rayleigh part of the first tap appropriately, allowing the 'method of moments' derived K-factor to be accurately represented.

Also generated are average delay and delay spread values for each matrix component. The latter are calculated in accordance with equation (8) earlier in this document.

An estimate of the 4-by-4 correlation matrix **R** is also created, based on the Rayleigh fading taps 2-18. It is assumed that the Rayleigh component of tap 1 can be similarly modelled. It is calculated as the average value of the outer product $\mathbf{vec}(\mathbf{H}^T)\mathbf{vec}(\mathbf{H}^T)^T$.

[18] Although true for 1122, the 1221 model is re-scaled by a degree dependent on the cross-power ratio

Averaging strategy for model_1122, model_1221, K_1122, K_1221, and R

The totality of the data gathered at 10m is organised into ‘locations’ and ‘shunts’, there being a variable number of shunts at each location (typically. 1-4).

At each location, all the shunt data is directly combined without normalisation. From it, a normalised set comprising *model_1122(l), model_1221(l), K_1122(l), K_1221(l)* and **R** is produced. Next, the mean of each of the normalised models *model_1122(l), model_1221(l), K_1122(l), K_1221(l)* and **R** is taken over all locations *l* to produce the final result. Only then are values converted to dB, where appropriate. The cross-power ratio is defined at each location by

XPR=(win_h11_power+win_h22_power)/(win_h12_power+win_h21_power)

Where ‘win_hxx_power’ denotes the total power in a Hann-windowed response hxx. The normalised average energy in the impulse response is 1 and 1/XPR for the principal terms and cross-terms respectively. The final result for the cross-power ratio is defined as 1/(mean(*model_1221*(*l*))) where *model_1221*(*l*) is the cross-term model at the *l*th location.